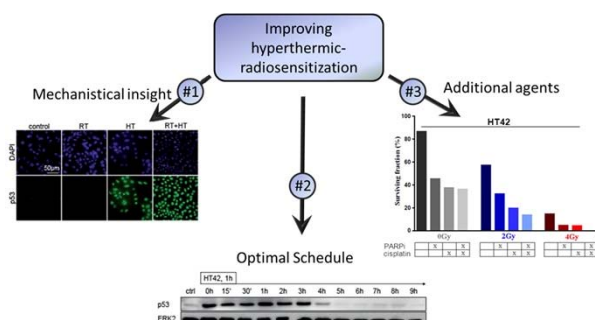


Purpose or Objective: Hyperthermia (raising the tumour temperature to 40-43°C) is an effective treatment in combination with radiotherapy for several tumour sites, including cervical cancer, which is mainly caused by infection with the Human Papillomavirus (HPV). The aim of our study is to improve treatment strategies for cervical carcinoma by (#1) unravelling mechanisms of hyperthermia induced radiosensitization, (#2) optimization of time interval between hyperthermia and radiotherapy and (#3) investigating the benefit of additional treatments.

Material and Methods: HPV-positive cervical cell lines SiHa and HeLa were used. Cells were treated with (#1) hyperthermia alone (42°C for 1h), (#2) hyperthermia and irradiation in different time intervals between the two therapies and (#3) hyperthermia and radiation with additional agents PARP1-inhibitor (i.e. a drug blocking a DNA repair protein) and cisplatin. Clonogenic survival assays and γH2AX stainings (a staining to visualize DNA double strand breaks) were carried out in order to determine the effectiveness of the (combined) treatments. Protein levels of p53 and DNA repair proteins were investigated using western blot. Apoptosis was measured in cell lines using the Nicoletti assay and cell cycle distribution was analyzed using the BrdU-assay.

Results: (#1) The high-risk HPV types 16 and 18 produce the oncoprotein, early protein 6 (E6), which binds to p53 before both proteins get degraded. Therefore, p53 cannot induce cell cycle block nor apoptosis, limiting the radiation effects. Hyperthermia increases the effectiveness by preventing the formation of the E6-p53 complex, rescuing p53 from degradation, resulting into functional p53 causing apoptosis and cell cycle arrest. (#2) Higher levels of p53 are present immediately after hyperthermia and remain up to four hours after treatment. The main therapy, radiotherapy or chemotherapy, should be applied within this time frame to yield a beneficial effect. (#3) Combination treatment of radiotherapy, hyperthermia, cisplatin and PARP1-inhibitors resulted in a lower survival fraction due to an increased number of DNA double strand breaks as compared to radiation alone. Cisplatin and PARP1-inhibition significantly enhanced the combined hyperthermia/radiation treatment.



Conclusion: Our findings provide new insights for patients suffering from HPV-positive cervical cancer. Hyperthermic-radiosensitization, makes radiotherapy significantly more effective by rescuing p53 from getting degraded. Adding PARP1-inhibitor or cisplatin further improves the effectiveness of hyperthermic-radiosensitization, which will increase clinical outcomes substantially.

EP-2025

The potential role of gold nanoparticles in proton beam radiosurgery for arteriovenous malformations

A. Nor¹, M. Morris¹, F. Vernimmen¹, M. Shmatov²

¹Cork University Hospital, Radiation Oncology, Cork, Ireland Republic of

²Ioffe Institute, Theoretical Physics, St Petersburg, Russian Federation

Purpose or Objective: To theoretically evaluate therapeutic gain from radiation dose enhancement by gold nanoparticles (AuNP) based on their physical interaction with protons.

Material and Methods: Nanoparticles range in size from 1 x 10⁻⁹m to 100 x 10⁻⁹m, and exert their effect by either entering the cell, or by attaching to the cell membrane surface. Radiation enhancement by gold nanoparticles (AuNP) is based on the generation of much localized secondary radiation when irradiated. This results in a Dose Enhancement Factor (DEF) and has been well described for photon irradiation and is most pronounced with kilo voltage photons, but happens also with Mega Voltage (MeV). For protons the DEF obtained with metallic nanoparticles has recently been studied. We took the definition of DEF as being: DEF = (D_{pure} + D_{GNP} - D_{wp}) / D_{pure}, where D_{pure} is the dose deposited in pure water.

Results: In vivo studies on tumors in mice have shown a considerable delay in tumor growth for mice receiving AuNPs with protons compared to protons alone. Protons have a high cross-section for gold over a large range of clinical energies, and the interaction produces Auger electrons with a very short range. The sphere of DEF around the AuNP is influenced by its size. For an AuNP of $r = 22\text{nm}$ and 80 MeV protons the radius of the sphere of DEF is in the order of 18nm, with dose enhancement factors of up to 2 described. We obtained a value of 1.06 at 1 nm from a nanoparticle with radius 25 nm and taking D_{pure} as being: D_{pure} [Gy] = 8.16 x Sw [MeV x cm²/g], where Sw is the stopping power of water. This small radius means that in order to be effective the AuNPs need to be in very close contact with the target. In the treatment of AVMs the prime target is the endothelial cell. Angiogenesis occurring in AVMs is driven by endothelial cells stimulated by vascular angiogenic factors binding on cell membrane receptors. AVM endothelial cells over express these receptors compared to their counterparts in normal brain vessels. IMC-1121B, a human antibody to VEGFR2, when linked with an AuNP has the potential to selectively increase the local AuNP concentration on the membrane of AVM endothelial cells. For conventional dose/fractionation schedules the radiobiological effects are governed by DNA damage in the cell nucleus. Membrane location could also be exploited because a cell membrane initiated effect is described, whereby activation of the acid sphingomyelinase/ceramide pathway occurs after doses >10 Gy, leading to endothelial apoptosis.

Conclusion: Successful AVM radiosurgery is amongst others dose dependent. Therapeutic gain in proton radiosurgery is possible with AuNP-VEGFR2ab located on the cell membrane, combined with doses > 10 Gy. This approach needs to be researched further, but offers the possibility for better obliteration rates and/or shorter latent intervals.

EP-2026

Effect of PARP-1 inhibition on human soft tissue sarcoma cells radiosensitivity

M. Mangoni¹, M. Sottili¹, C. Gerini¹, I. Meattini¹, I. Desideri¹, P. Bono¹, D. Greto¹, M. Loi¹, R. Capanna², G. Beltrami², D. Campanacci², L. Livi¹

¹University of Florence, Experimental and Clinical Biomedical Sciences, Firenze, Italy

²Careggi University Hospital, Department of Orthopaedic Oncology, Florence, Italy

Purpose or Objective: Soft-tissue sarcomas (STS) are aggressive tumours with a poor prognosis and there is a major clinical need for novel strategies. Poly-ADP ribose polymerase (PARP)-1 promotes base excision repair and DNA strand break repair. Inhibitors of PARP (PARPi) have shown to enhance the cytotoxic effect of irradiation (IR), and evidences suggest that PARPi could be used to selectively kill cancers defective in DNA repair. Sarcomagenesis is linked to aberrant biological pathways and some STS have defect in DNA repair systems, so there is a rationale for using PARPi in STS. We investigated the effect of PARP inhibition on STS cell lines survival after IR and on radiation-induced DNA damage foci.

Material and Methods: Cell proliferation analysis was performed on human fibrosarcoma, liposarcoma, leiomyosarcoma and rhabdomyosarcoma cell lines with increasing doses of olaparib (0.25; 0.5; 1; 2; 4 μ M) 3 h after cells seeding. The numbers of cells were assessed after 5 days and results normalized to the untreated control. For clonogenic assays, fibrosarcoma, liposarcoma, leiomyosarcoma and rhabdomyosarcoma cells were irradiated with 2, 4 or 6 Gy, with or without olaparib (1 μ M) iniparib (10 μ M) or veliparib (5 μ M) pre-treatment. The plating efficiency of the combined treatments were normalized to PARPi-treated cells. The linear-quadratic survival expression was fitted to the data by nonlinear regression. The radiosensitization enhancement ratio for the PARPi at 50% survival (ER50) was as follows: ER50 = Dose at 50% survival without PARPi/Dose at 50% survival with PARPi. The impact of PARP inhibition on γ -H2AX foci formation was evaluated in rhabdomyosarcoma cells treated with olaparib 1 μ M after 48 h, and irradiated at 4 Gy. Cells were probed with primary antibody to γ -H2AX.

Results: Continuous treatment with olaparib for 5 days resulted in a dose-dependent inhibition of proliferation in all the STS cell lines. Significant radiosensitization was observed in all human STS cell lines using PARPi, with an ER50 ranging from 1.2 to 3.41. Rhabdomyosarcoma showed the greatest increase in radiosensitivity, with an ER50 of 3.41 with veliparib. Fibrosarcoma showed an ER50 of 2.29 with olaparib and 2.21 with veliparib. Leiomyosarcoma and liposarcoma showed similar radiation responses after PARP inhibition, with the higher radiosensitization in presence of veliparib (ER50 1.62 and 1.46, respectively). The combination of olaparib and radiation in rhabdomyosarcoma cells resulted in an increased number of γ H2AX foci as compared to control and irradiation alone.

Conclusion: We demonstrated that PARPi are potent radiosensitizers on human STS in vitro models. The different PARPi radiosensitizing effects observed in various cell lines may be explained by the presence of different genomic aberrations in DNA repair machinery in specific STS subtypes. These preliminary data encourage to further study association of PARPi with IR as a promising treatment for STS.

EP-2027

Fractionated radiotherapy plus anti-angiogenic therapy in an orthotopic glioma transplantation model

V. Albrecht¹, J. Schuster¹, M. Proescholdt², D. Piehlmaier³, K. Unger³, C. Belka¹, M. Niyazi¹, K. Lauber¹

¹LMU Munich, Clinic for Radiotherapy and Radiation Oncology, Munich, Germany

²University Hospital Regensburg- Germany, Department of Neurosurgery, Regensburg, Germany

³Helmholtz Center Munich - German Research Center for Environmental Health GmbH- Neuherberg- German, Research Unit of Radiation Cytogenetics, Neuherberg, Germany

Purpose or Objective: Glioblastoma (GBM) is the most common primary brain tumor in adults. Despite intense treatment, including surgery and radiochemotherapy, prognosis is dismal with a median overall survival time of only 15 months. The vascular endothelial growth factor-A (VEGF-A) has been identified as one of the key regulators of neoangiogenesis in these highly vascularized tumors. Therefore, disruption of the VEGF-A signaling cascade by neutralizing VEGF-A and preventing ligation of its receptors appeared to be a promising approach for targeting neoangiogenesis. However, in recent phase III trials application of the VEGF-A blocking antibody bevacizumab in combination with radiochemotherapy failed to prolong overall survival in newly diagnosed GBM despite increasing progression-free survival and improving performance status. The aim of our study was to analyze the treatment effects of radiotherapy in combination with bevacizumab in a clinically relevant setting. Therefore, we established an orthotopic, syngeneic mouse glioblastoma model and subjected it to fractionated radiotherapy in combination with the bevacizumab mouse analogue G6-31.

Material and Methods: GL261 mouse GBM cells were stereotactically transplanted into the frontal lobe of C57/BL6 mice and tumors were allowed to grow for one week. Radiation therapy was performed with a Small Animal Radiation Research Platform (SARRP, Xstrahl) which incorporates contrast agent-CT (CA-CT)-based imaging followed by high precision radiation delivery. Fractionated irradiation with daily doses of 2 Gy up to a cumulative dose of 20 Gy was administered with or without accompanying VEGF-A blockade by the mouse bevacizumab analogue G6-31. Overall survival and tumor size were monitored, histological analyses, and transcriptomic profiling of tumor and normal tissue are currently being performed.

Results: Stereotactic implantation of GBM was successfully accomplished, fractionated irradiation was implemented by CA-CT-based image guidance, and tumor growth was successfully monitored by serial CA-CT scans. The single agent treatments led to a significant delay in tumor growth and prolongation of survival as compared to the sham-treated controls. Importantly, the strongest therapeutic effects were observed with the combined treatment. Histological details, including vessel density and structure, as well as markers of cell death induction, and transcriptomic profiling of tumor and normal tissue are currently under investigation.

Conclusion: This pilot study shows that syngeneic, orthotopic glioblastoma transplants combined with stereotactically delivered radiotherapy are feasible and clinically relevant in vivo models for evaluating the therapeutic efficacy of multimodal treatment approaches based on fractionated irradiation.

EP-2028

Dependence of dose enhancement on the cluster morphology of Gold Nano Particle in radiation therapy

A. Sang Hee Ahn¹, C. Kwangzoo Chung², H. Youngyih Han², P. Hee Chul Park², C. Doo Ho Choi²

¹Sungkyunkwan University, Department of Health Sciences and Technology- Samsung Advanced Institute for Health Sciences and Technology, Seoul, Korea Republic of

²Samsung Medical Center, Sungkyunkwan University School of Medicine Radiation Oncology, Seoul, Korea Republic of

Purpose or Objective: Injected gold nano particles(GNPs) to a body for dose enhancement are known to form cluster morphology. We investigated the dependence of dose enhancement on the morphology characteristic with an approximated morphology model by using Monte Carlo simulations.

Material and Methods: For MC simulation, TOPAS v.b-12 was used. GNPs of 50 and 100 nm diameter were tested. GNP cluster morphology was approximated as a body center cubic by placing 8 GNPs at the corner and one at the centered of a $2 \times 2 \times 2 \mu\text{m}^3$, $1 \times 1 \times 1 \mu\text{m}^3$, $0.5 \times 0.5 \times 0.5 \mu\text{m}^3$, or $0.25 \times 0.25 \times 0.25 \mu\text{m}^3$ (for 100 nm GNP) or $0.18 \times 0.18 \times 0.18 \mu\text{m}^3$ (for 50 nm GNP) cube located in a $4 \times 4 \times 4 \mu\text{m}^3$ water filled cube phantom. $4 \mu\text{m} \times 4 \mu\text{m}$ square shaped beams of spectrum-energetic 50, 100 kVp photons and 70, 170 MeV protons were irradiated to the water filled cube phantom with GNPs in it. We computed the distribution of secondary electrons as a function of distance from the surface of the GNP at the cube center and calculated the ratio (SER) together with dose enhancement ratio (DER) for 4 different cubes geometries. For scoring particles, 10 nm width of concentric shell shaped detector was constructed up to 100 nm from the center point of the cube. 10^8 histories of protons and 2×10^{10} histories of photons were used for simulation. All counted values at each detector were summed to obtain the total dose and secondary electrons in a sphere of 100 nm radius and were normalized to $2 \times 2 \times 2 \mu\text{m}^3$ cube morphology.